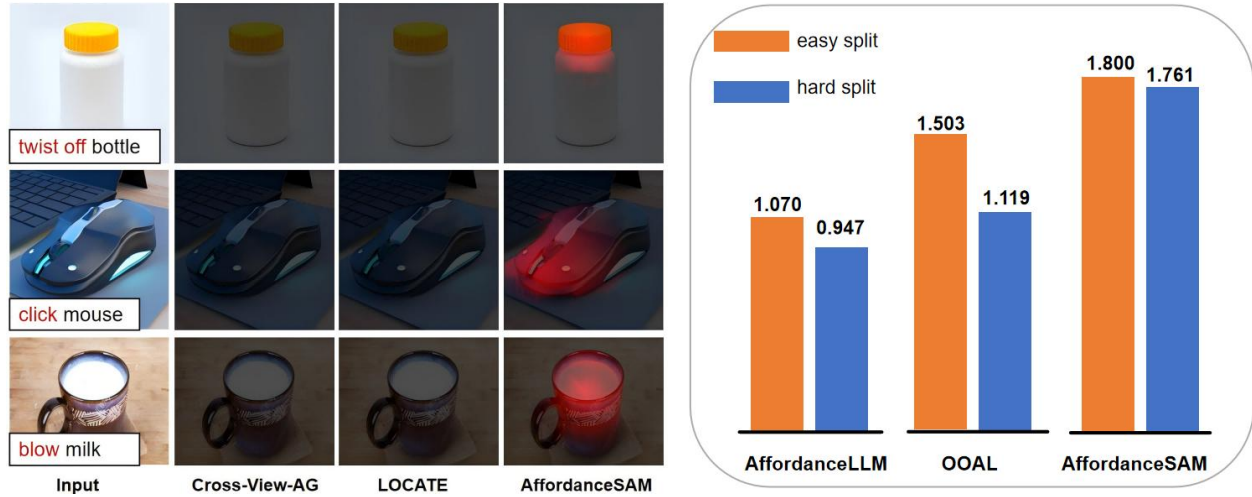


AffordanceSAM: Segment Anything Once More in Affordance Grounding

Dengyang Jiang^{1,2*} Mengmeng Wang^{3,2†} Teli Ma⁴
 Hengzhuang Li^{5,2*} Yong Liu⁶ Guang Dai² Lei Zhang¹

¹ NWPU ² SGIT AI Lab ³ ZJUT ⁴ HKUST(GZ) ⁵ HUST ⁶ ZJU



(a) Generalization results on **novel** affordance functions marked in red. We do not highlight any region when the model can not infer.

(b) NSS metric results under AGD20K benchmark.

Figure 1. **Left:** Compared to the weakly supervised methods that can not infer novel affordance function, our AffordanceSAM showcases open affordance vocabulary understanding ability and provide very reasonable affordance maps. **Right:** Compared to other fully supervised methods, our AffordanceSAM outperforms them in a large margin. More importantly, our approach can still sustain the performance despite testing samples are significantly different from the training objects, which also prove the robustness of our proposed AffordanceSAM.

Abstract

Improving the generalization ability of an affordance grounding model to recognize regions for unseen objects and affordance functions is crucial for real-world application. However, current models are still far away from such standards. To address this problem, we introduce AffordanceSAM, an effective approach that extends SAM’s generalization capacity to the domain of affordance grounding. For the purpose of thoroughly transferring SAM’s robust performance in segmentation to affordance, we initially propose an affordance-adaption module in order to help modify SAMs segmentation output to be adapted to the specific functional regions required for affordance grounding. We concurrently make a coarse-to-fine training recipe to make SAM first be aware of affordance objects and actions coarsely, and then be able to generate affordance heatmaps

finely. Both quantitative and qualitative experiments show the strong generalization capacity of our AffordanceSAM, which not only surpasses previous methods under AGD20K benchmark but also shows evidence to handle the task with novel objects and affordance functions.

1. Introduction

Affordance grounding [12, 15] refers to finding potential action possibilities regions of an object, which plays a pivotal role in bridging the gap between visual perception and robotic action. Recently, attempts [24, 25, 29, 34, 38, 39] made to endow models to have the ability to ground objects can be broadly divided into two methodologies. The first type of methods is weakly supervised affordance grounding [24, 29, 34], which aims to make the right classifications on the predefined affordance classes by extracting affordance-related knowledge from different centric views.

*Work was done during internship at SGAI.

†Corresponding author

The affordance maps are obtained via class activation mapping (CAM) [56]. However, these methods completely break down when facing new affordance functions as their supported classes are fixed. To tackle this problem, the second type of methods uses affordance maps to directly supervise the models [25, 38, 39]. However, the brittle affordance components trained from scratch on the hundreds of pieces manually labeled training data make it insufficient to obtain a highly generalized model. To this end, we raise a question: *How can we obtain a model with generalization ability under such limited data conditions?*

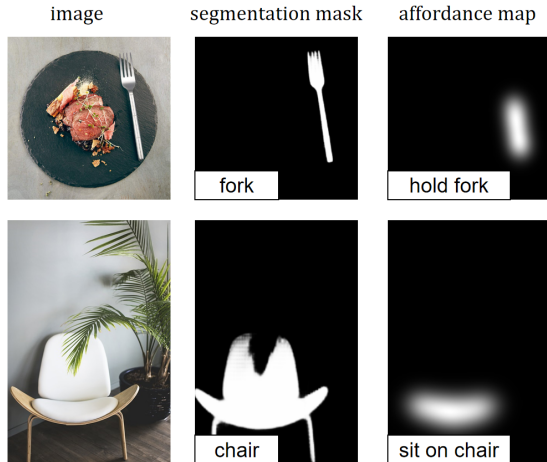


Figure 2. **Visualization of differences between segmentation and affordance**, where segmentation focuses on separating objects directly according to the prompt, but affordance emphasizes grounding the possible effective part of objects based on the affordance query.

In this work, we try to decompose and answer the above question in a step-by-step manner:

(i) Can we incorporate a suitable and generalized vision prior? With the recent advancements in large-scale pre-trained foundation models, many works have attempted to leverage the prior knowledge for downstream task transfer [14, 18, 47, 53]. We believe this paradigm is also effective for affordance grounding task. Given that affordance grounding inherently requires pixel-level localization, we explore the possibility of incorporating SAM (Segment Anything Model) [20, 41] since SAM not only demonstrates remarkable generalization capabilities but also excels in precise object localization after pre-trained on large-scale masked-labeled data. Moreover, the model structure and decoder output format of segmentation and affordance grounding are highly similar. Considering these similarities between segmentation and affordance grounding, we hypothesize that incorporating SAM could be both promising and well-suited for our problem.

(ii) How can we effectively utilize and transfer SAM’s comprehensive knowledge into affordance grounding task?

Although there are some similarities between segmentation and affordance grounding, task differences still exist. As shown in Figure 2, firstly, affordance grounding requires the recognition of functional parts of objects based on verb queries, while segmentation only requires the separation of complete objects; next, the ground-truth of segmentation and affordance differs slightly: the former uses a binary mask, while the latter uses a heatmap that encodes functional possibilities. To address these two primary challenges, we propose a simple but efficient framework from model structure to specific training recipe to obtain an affordance version of SAM, termed as AffordanceSAM.

Specifically, we initially design an affordance-adaption module that utilizes learnable queries to interact with text and image features, these queries are then sent into the decoder to refine the original mask produced by SAM. We assume that this prompt learning-like [57] lightweight module can effectively search for affordance-relevant parts in the comprehensive knowledge of SAM. We then make a three-stage training recipe that employs a coarse-to-fine approach. In the first stage, we curate a coarsely mask-labeled dataset by merging and reclassifying existing datasets, focusing on object-affordance pairings. This enables the model to learn basic object-verb relationships. After that, we use a weakly supervised model to generate pseudo-labels for unannotated images and post-process them to supervise our model. Finally, we further fine-tune the model on the high-quality, human-labeled data for finer affordance map generation.

In summary, our contributions are as follows:

- We innovatively incorporate SAM for affordance grounding, empowering our model to generalize effectively beyond the training data.
- We simultaneously introduce an affordance-adaption module and coarse-to-fine training recipe to effectively utilize and transfer SAM’s comprehensive knowledge into affordance grounding.
- In our comprehensive experiments, our model achieves state-of-the-art (SOTA) performance under the AGD20K benchmark, and shows evidence to generalize well to novel actions and objects.

2. Related Work

We discuss with the most relevant studies here and provide a more discussion in Appendix 1.

Affordance grounding. Different from well-known detection [55] and segmentation [32] that acquire the model to output bounding box and binary mask of the desired objects, affordance grounding task [12, 15] needs model to output heatmap that encodes functional possibilities in a object. At the beginning, there are some works [31, 34, 36] tried to equip the model of such capacity. But because the data restriction at that time, these models can only recognize a few types of objects and actions. Next, Luo *et al.* collect

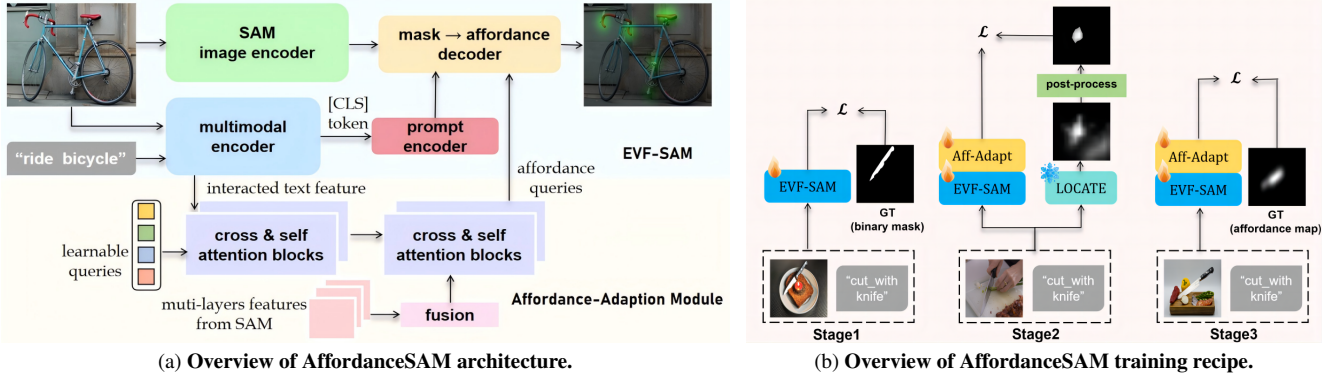


Figure 3. **(a). Architecture:** AffordanceSAM is built upon EVF-SAM [52] with an additional affordance-adaption module. The inputs of our model include a single image and a text prompt related to interaction. In our affordance-adaption module, we employ learnable queries to fuse with text feature and multiple layers of features from SAM encoder and then incorporate them into the original decoder to help the transformation from mask to the final affordance map. **(b). Training:** AffordanceSAM adopts a coarse-to-fine training recipe. In stage1 and stage3, we use ground truth binary masks and affordance maps to supervise the model, respectively. In stage2, affordance maps output by LOCATE and then pass through our proposed post-process program are used to supervise the model.

the first large-scale affordance dataset called AGD20K [29] and annotated a few of the data with affordance maps (1675/23816). After that, many works [24, 25, 39] engined by AGD20K have emerged. For example, LOCATE [24] localizes and extracts affordance-specific information in exocentric and transfers this knowledge to egocentric in a weakly supervised manner; OOAL [25] builds a vision-language learning framework based on CLIP [40] and DINOv2 [35] to conduct one-shot open affordance learning. However, non of above works shows satisfactory generalization ability to recognize regions for unseen objects and affordance functions (reasons are explained in Section 1 and evidences are shown in our experiment results). In this study, we aim at utilizing SAM as base model with our proposed transferring approach to build a generalized affordance grounding model to fill this gap.

Adapting foundation model to downstream task. Vision foundation models (e.g. SAM [20], CLIP [40], DINOv2 [35]) are large-sized models trained over a vast amounts of data. After training, they are suitable to be a start point for variety of downstream tasks under limited data condition. Recently, many works have attempted to leverage different foundation models for different downstream tasks [14, 18, 47, 53]. For example, ActionCLIP [47] proposes pre-train, prompt and fine-tune strategy to transfer CLIP to action recognition aspect; FM-FSOD [14] use DINOv2 to extract fine-grained features for few-shot object detection. Our work also share similarities, while we focus on adapting SAM to affordance grounding task with our proposed affordance-adaption module and coarse-to-fine training recipe.

3. Approach

The overall model architecture and training procedure of AffordanceSAM are shown in Figure 3a and Figure 3b.

As our model consists of two primary components: the EVF-SAM [52]¹ baseline and the affordance-adaption module, we begin with describing each in Section 3.1 and Section 3.2. Finally, in Section 3.3, we provide a comprehensive elucidation of our coarse-to-fine training recipe.

3.1. Preliminary

Baseline EVF-SAM. As we need to provide text prompts that contain affordance queries to the model but original SAM lacks language understanding abilities. We choose to start from EVF-SAM [52] which is the state-of-the-art method among attempts [23, 42, 52, 54] that explored SAM to segment objects according to the text instructions. We seek to leverage its robust segmentation capabilities for affordance grounding.

The EVF-SAM original framework incorporates four key components: a multimodal encoder (BEIT-3 [48]) denoted as \mathcal{E}_M , a prompt encoder \mathcal{E}_P , a SAM image encoder \mathcal{E}_I , and a SAM mask decoder \mathcal{D} . The input image is firstly processed through two parallel paths: (i): conversion to SAM image tokens $\mathbf{I}_s \in \mathbb{R}^{B \times N_s \times D_s}$, and (ii): transformation to multimodal image tokens $\mathbf{I}_m \in \mathbb{R}^{B \times N_m \times D_m}$, where B represents batch size, N sequence length, and D feature dimension. Meanwhile, the text input is first tokenized to produce text tokens $\mathbf{T} \in \mathbb{R}^{B \times N_t \times D_m}$. These text and multimodal image tokens are then combined with a learnable [CLS] token $\in \mathbb{R}^{B \times 1 \times D_m}$ and processed by the multimodal encoder:

$$\mathbf{F}_m = \mathcal{E}_M([\text{CLS}]; \mathbf{I}_m; \mathbf{T}) \in \mathbb{R}^{B \times (1+N_m+N_t) \times D_m}. \quad (1)$$

The [CLS] token output \mathbf{F}_c which is split from \mathbf{F}_m is transformed by the prompt encoder, then together with the

¹EVF-SAM can be seen as an extension version of SAM that support text prompts. In this paper, we use term ‘EVF-SAM’ to refer the specific model part and ‘SAM’ for our general argument.

Stage	Data Source	Label Type	Num.
1	PADv2 / Handal / RGB-D Part Affordance	Binary Mask	39159
2	Unlabeled Part of AGD20K	Pseudo Labeled Affordance Map	13323 (Easy Split) 11889 (Hard Split)
3	Labeled Part of AGD20K	Human Annotated Affordance Map	1135 (Easy Split) 868 (Hard Split)

Table 1. **Overview of the training datasets for AffordanceSAM.** This table summarizes the data source, format of groundtruth, the number of samples for training in each stage. More details can be found in Appendix 2.

SAM encoded image features to generate binary mask \mathbf{M}_b :

$$\mathbf{M}_b = \mathcal{D}(\mathcal{E}_I(\mathbf{I}_s), \mathcal{E}_P(\mathbf{F}_c)). \quad (2)$$

3.2. Affordance-Adaption Module

As shown in Figure 2, there exists a substantial disparity between the output of the segmentation task and the affordance grounding task. To efficiently adapt SAM to the dataset labeled with affordance maps instead of its original output masks, we introduce this module. Similar to BLIP-2 [26] and DETR [8], we introduce a set of learnable queries termed affordance queries. These queries, denoted as $\mathbf{Q}_a \in N_s \times D_m$, first repeat over batch dimension and conduct cross-attention with the text features that interact with the image in the multimodal encoder. we expect these queries to extract information concerning the affordance function from these semantic features. What’s more, since different layers of SAM’s features often exhibit different levels of granularity and knowledge [17], and affordance may correspond to multiple parts of an object. We consider a diverse set of granularities can be beneficial. Therefore, the second cross-attention operation is performed between the processed affordance queries and fused visual features of SAM’s multiple layers formulated as:

$$\mathbf{F}v = \sum_{i=1}^j \alpha_i \cdot \text{Linear}(\mathbf{G}_i), \quad \alpha_1 + \dots + \alpha_j = 1, \quad (3)$$

where $\mathbf{G}_i \in \mathbb{R}^{B \times N_s \times D_s}$ denotes features from the global-attention blocks in SAM image encoder, α_i is a learnable parameter that controls the fusion ratio of each feature. It is worth noting that we also add one self-attention block after each cross-attention block for enhanced feature learning. The final affordance queries \mathbf{Q}_{af} are first processed by two transposed convolution functions to adjust the dimension, then added with mask features from the original EVF-SAM to obtain the modified features for final process. Thus, we can obtain the affordance map output \mathbf{M}_a as:

$$\mathbf{M}_a = \mathcal{D}(\mathcal{E}_I(\mathbf{I}_s), \mathcal{E}_P(\mathbf{F}_c), \text{TransConv}(\mathbf{Q}_{af})). \quad (4)$$

3.3. Coarse-to-Fine Training Recipe

In order to fully leverage SAM’s generalization capacity for affordance grounding, we elaborately crafted a coarse-to-fine training recipe shown in Figure 3b, which consists of

three stages. The overall training data is displayed in Table 1. In all stages, we use a template of “<affordance function> <object_name>”, for instance, “wear hat”, as the text prompt for AffordanceSAM. The detailed dataset setup are provided in Appendix 2.

Training stage1. In most training datasets for multimodal models and text-prompted segmentation models, such as LAION-400M [44], RefCLEF [16], and RefCOCO [50], there are very few objects with affordance properties and very little textual content that contains verbs. However, it is crucial for an affordance grounding model to familiarize itself with such objects and understand affordance verb information for locating potential action-possibilities regions. Based on the above observations, we decided to let EVF-SAM first meet this requirement from a coarse perspective without any change in output form. Therefore, we select three datasets, PADv2 [51], Handal [13], and RGB-D Part Affordance [33], which satisfy both objects contained with affordance functions and annotations of masks. We then combine them according to the categories of objects and affordance functions. We only use EVF-SAM baseline without the affordance-adaption module and fine-tune multimodal encoder and prompt encoder in this stage. The training loss function is given by

$$\mathcal{L} = \lambda_{dice} \cdot \mathcal{L}_{dice} + \lambda_{bce} \cdot \mathcal{L}_{bce}, \quad (5)$$

where the overall loss function \mathcal{L} is the weighted sum of DICE loss \mathcal{L}_{dice} [45] and BCE loss \mathcal{L}_{bce} [43], determined by λ_{dice} and λ_{bce} .

Algorithm 1 Affordance maps post-process algorithm in stage2.

Input: Affordance map M_{al} generated by LOCATE and threshold γ .

- 1: $\gamma_1 = \gamma \cdot \max(M_{al})$
- 2: $\gamma_2 = 0.4 \cdot \gamma_1$
- 3: $\gamma_3 = 0.2 \cdot \gamma_2$
- 4: $M_{ap} = \text{where}(M_{al} \geq \gamma_1, M_{al}, \frac{M_{al}^2}{\gamma_1})$
- 5: $M_{ap} = \text{where}(M_{ap} \geq \gamma_2, M_{ap}, \frac{M_{ap}^2}{\gamma_2})$
- 6: $M_{ap} = \text{where}(M_{ap} \geq \gamma_3, M_{ap}, 0)$

Output: Processed affordance map M_{ap} .

Method	Venue	Easy Split			Hard Split		
		KLD↓	SIM↑	NSS↑	KLD↓	SIM↑	NSS↑
Cross-View-AG [29]	CVPR'22	1.787	0.285	0.829	2.092	0.209	0.138
LOCATE [24]	CVPR'23	1.405	0.372	1.157	1.829	0.282	0.276
AffordanceLLM [39]	CVPR'24	1.463	0.377	1.070	1.661	0.361	0.947
OOAL [25]	CVPR'24	1.070	0.461	1.503	1.302	0.410	1.119
AffordanceSAM _{SAM1}	this work	<u>1.083</u>	0.543	1.800	1.128	0.514	1.761
AffordanceSAM _{SAM2}	this work	1.141	<u>0.530</u>	<u>1.631</u>	<u>1.214</u>	<u>0.496</u>	<u>1.536</u>

Table 2. **Quantitative results on the Easy split and Hard Split of AGD20K.** The best and second-best results are highlighted in bold and underlined. *SAM1* and *SAM2* denote different versions of SAM backbones (SAM-ViT-H [20] and SAM2-hiera-L [41]) for initialization.

Training stage2. As mentioned in Section 1 and Table 1, images with dense pixel labeling affordance maps are scarce and it can be costly for us to annotate. In practice, we find that training only on the hundreds of labeled images could not fully convert SAM’s output mask into an affordance map. Hence, we utilize the state-of-the-art weakly supervised model on AGD20K, LOCATE [24], to label the vast majority of the remaining unlabeled images in AGD20K. However, The raw output affordance heatmaps of LOCATE are usually suboptimal, which exist a large area of low thermal regions unrelated to the target. Hence, we design a post-processing program showed in Algorithm 1 to mitigate such issue. These processed pseudo labels help bridge the gap between binary segmentation masks from stage1 and the detailed affordance heatmaps needed for the final output, serving as an intermediate step in our coarse-to-fine training pipeline. During training, we add affordance-adaption module and keep only SAM image encoder frozen. we follow AffordanceLLM [39] to use binary focal loss [27] (\mathcal{L}_{focal}) and set the weight of positive examples to be 0.9 and that of negative ones to be 0.1, as there are often more negatives than positives in an affordance map.

Training stage3. In this stage, we use the high-quality human-labeled samples in AGD20K to supervise the model. We aim at regulating the model to generate the most precise and fine-grained affordance maps. We keep the loss function and trainable modules unchanged compared to stage2.

4. Experiments

4.1. Experimental Setup

Implementation details. In stage1, we initialize our AffordanceSAM with EVF-SAM [52] and train for 13 epochs with base learning as 0.00002. In stage2, we use the weights obtained from the first stage and randomly initialize affordance-adaption module, we train the model with the same number of epochs and base learning as stage1. In stage3, we further train our model for 26 epochs with larger base learning as 0.00004. In all training stages, we employ an AdamW optimizer [19] with a cosine learning rate

scheduler, and the total batchsize per iteration is 32 using 4 NVIDIA A100 (80GB) GPUs.

Evaluation. We follow AffordanceLLM [39] to have two splits (easy split and hard split) of AGD20K to test our model. The easy split is the original unseen split of AGD20K, which has a lot of similarities between the objects in the train and test sets. The hard split ensures that there is no overlap between the object categories in the train and test set (both in our stage 2 and stage 3). Meanwhile, we follow the metrics provided in AGD20K to evaluate our model, which is Kullback-Leibler Divergence (KLD) [7], Similarity (SIM) [46] and Normalized Scanpath Saliency (NSS) [37]. For KLD, the lower the better, and for SIM and NSS, the higher, the better.

Methods for comparison. As we indicate in Section 1, affordance grounding methods can be mainly summarized into two main categories: weakly supervised and fully supervised methods. We compare our approach against representative weakly supervised baselines (Cross-View-AG [29] and LOCATE [24]), and fully supervised baselines (AffordanceLLM [39] and OOAL [25]). we do not conduct the qualitative comparison with AffordanceSAM because it is not open-source and lacks sufficient implementation details to be reproduced.

We also provide more details about our implementation including training hyperparameters and model configuration, details of each metric, and detailed descriptions of each baseline method for comparison in Appendix 3~5.

4.2. Main Results

Quantitative Results on AGD20K. Table 2 presents the quantitative results of our proposed AffordanceSAM alongside other baselines on both the easy split and hard split of the AGD20K. Our AffordanceSAM, particularly the SAM1 variant, demonstrates superior performance across multiple metrics. On the easy split, it achieves the highest scores in SIM (0.543) and NSS (1.800). Most importantly, the advantages of our approach become more pronounced on the challenging hard split, where the objects in the test set bear little to none resemblance to the ones in the training set. To be

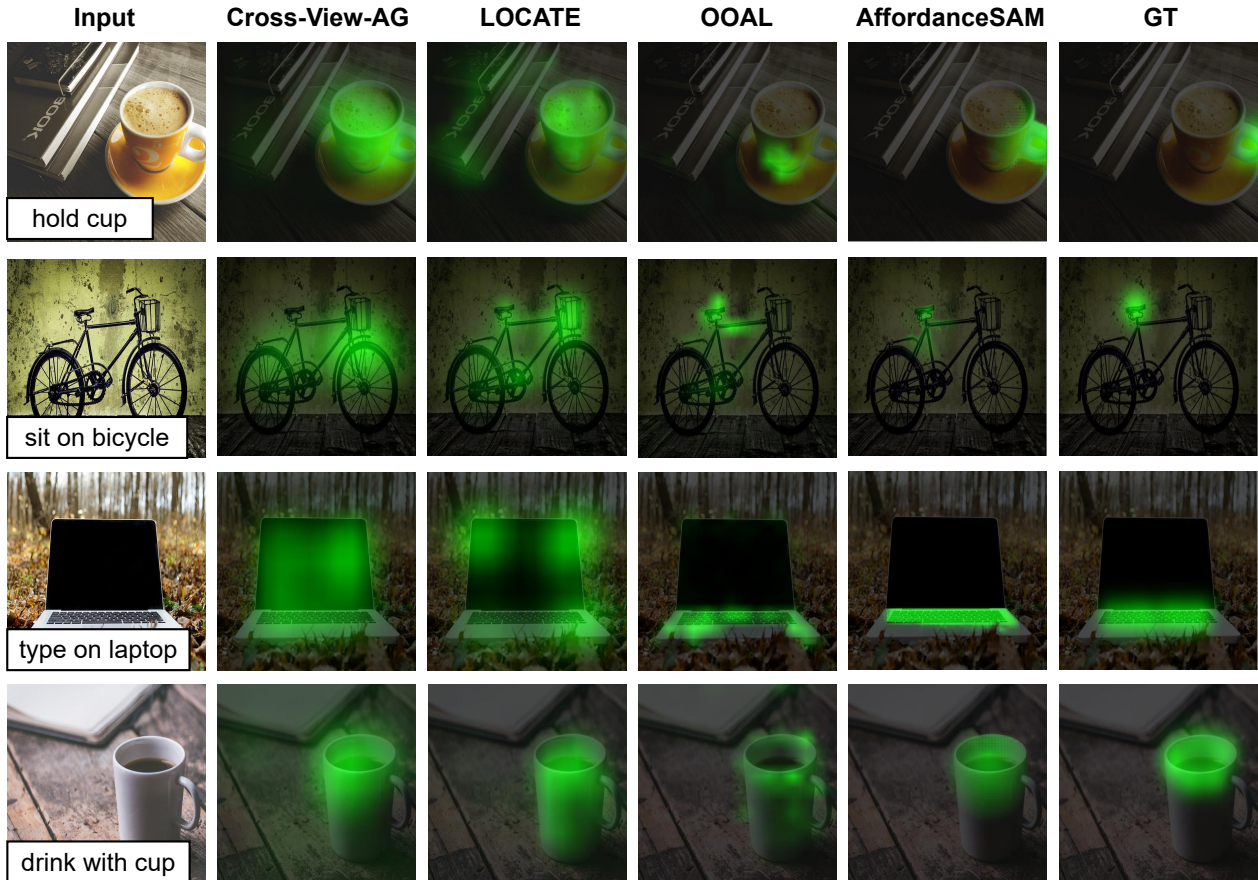


Figure 4. **Qualitative comparison with other methods on AGD20K dataset.** Cross-View-AG and LOCATE often make affordance predictions with a large area of low thermal regions unrelated to the target. On the contrary, OOAL focuses on a small area but sometimes it’s completely wrong. Our AffordanceSAM can precisely recognize the part of the object that contains the affordance function.

specific, both two versions of AffordanceSAM achieve superior performance, and our best version reduces the KLD by 17.4%, while simultaneously increasing the SIM and NSS scores by 10.4% and 64.2% respectively when compared to the previous best performing method OOAL [25]. This delightful result suggests that our method successfully inherits SAM’s strong generalization ability and generalizes well to more challenging scenarios.

Qualitative Results on AGD20K. As shown in Figure 4, we present four examples from the validation set of AGD20K to see how AffordanceSAM outperforms other methods. For instance, when handling the object “cup”, AffordanceSAM demonstrates a superior understanding of affordance functions compared to other methods and generates more accurate and precise affordance maps according to different actions “hold” and “drink”. Furthermore, benefiting from SAM’s ability to accurately segment objects at the pixel level, our AffordanceSAM can sometimes give even more precise affordance maps than the ground-truth (see the middle two lines of Figure 4).

Qualitative Results on Internet Images. To further demonstrate the generalization capacity of Affordance-

SAM, we also present qualitative comparisons when facing new objects selected from the internet. As we can see, AffordanceSAM not only produces very reasonable affordance maps for learned affordance functions showed in the first three rows of Figure 5, but is also able to handle novel actions presented in the last three rows of Figure 5. By contrast, understanding new actions is beyond the capability of Cross-View-AG and LOCATE, and OOAL can not make concentrated predictions for things beyond training data. These results substantiate that our AffordanceSAM can benefit so greatly from the foundation model SAM, thus showcasing leading affordance grounding performance towards novel objects and affordance functions.

4.3. Ablation Study

In this section, we conduct an extensive ablation study to reveal the contribution and design-space of each component. Unless otherwise specified, we report the results on hard split of AffordanceSAM_{SAM1} using our default settings. Please refer to Appendix 6 to see the detailed illustration of the evaluation setup of each table.

Contribution of Coarse-to-Fine Training Recipe. As

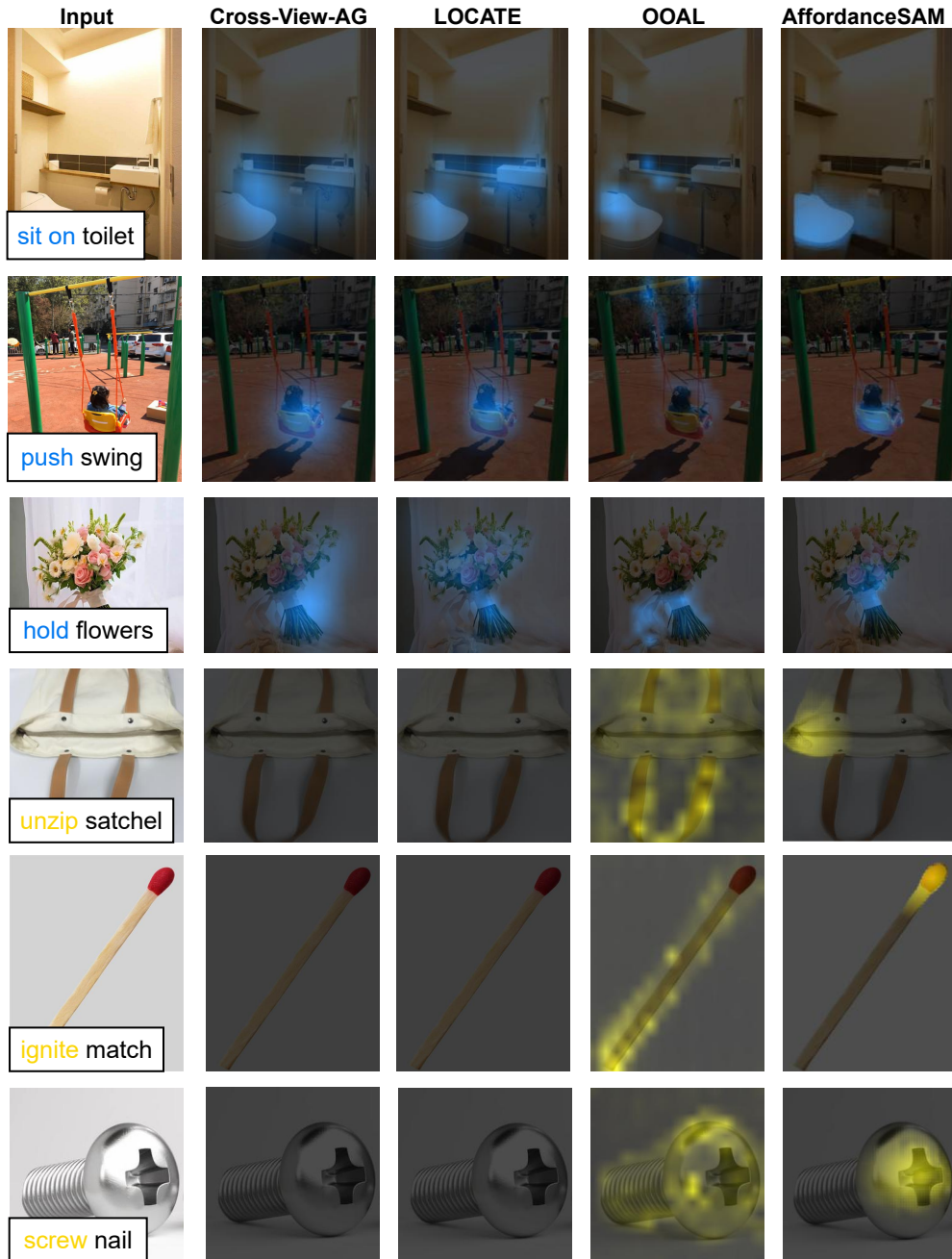


Figure 5. **Qualitative results with novel objects from the internet.** **learned** and **novel** affordance functions are marked in blue and yellow. Cross-View-AG and LOCATE can not generalize to new affordance functions, so we do not highlight any region. OOAL often outputs suboptimal affordance maps when encountering new objects and affordance functions. By contrast, our AffordanceSAM can still give reasonable affordance maps.

depicted in Table 3, our proposed coarse-to-fine training recipe demonstrates a clear performance enhancement. It is noteworthy that directly employing EVF-SAM to assess results can be highly unsatisfactory (see the first row), which is consistent with the analysis in Section 1 and Figure 2 that SAM lacks the capability to recognize affordance verbs and thereby overly segments objects. Encouragingly, after our

three consecutive stages of training in a stepwise manner, it can be found that the affordance performance has been progressively enhanced. Moreover, as shown in the last row, directly combining all the data can lead to worse result, this may be because directly mixing different quality of data and ground-truth format causes the performance degeneration, which is consistent with the observations in tuning LLMs

Stage1	Stage2	Stage3	KLD ↓	SIM ↑	NSS ↑
×	×	×	2.924	0.184	0.115
✓	×	×	2.280	0.289	0.741
✓	✓	×	1.592	0.396	1.319
✓	✓	✓	1.128	0.514	1.761
Combining all the data			1.735	0.361	1.265

Table 3. **Ablation results of coarse-to-fine training recipe.** First, we gradually add the training data divided by stage. Then, we provide the results when directly combine all the data and train for one stage.

Modules	KLD ↓	SIM ↑	NSS ↑
EVF-SAM only	1.327	0.422	1.615
w/ LQ	1.221	0.475	1.695
w/ LQ, F_t	1.218	0.487	1.703
w/ LQ, F_t, F_v w/ m	1.128	0.514	1.761
w/ LQ, F_t, F_v wo/ m	1.192	0.503	1.749

Table 4. **Ablation results of affordance-adaption module.** LQ : learnable queries. F_t : interaction with text feature. F_v w/ m: interaction with fused image features. F_v wo/ m: interaction with only last layer image feature.

Table 7. **AffordanceSAM ablation experiments on the hard split.** The default setting is marked in gray.

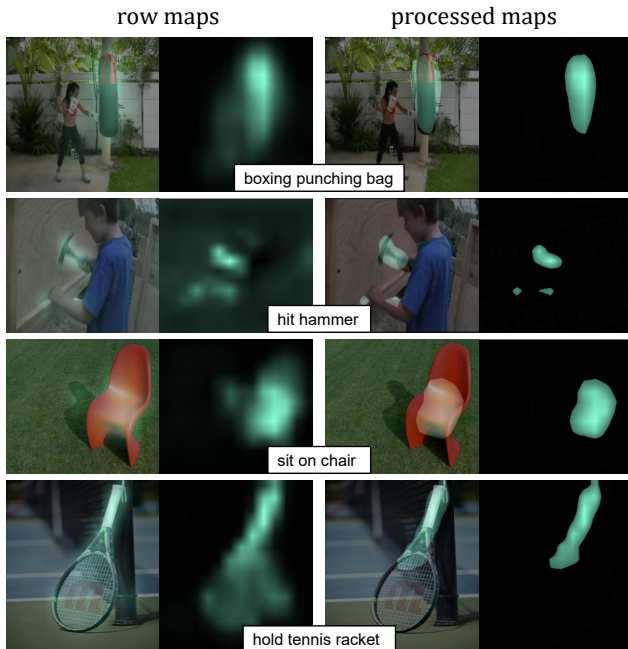


Figure 6. **Visual comparison between row affordance maps and our processed maps.** It is apparent that our post-processing program successfully mitigate some low thermal regions of the row affordance maps output by LOCATE.

to MLLMs [4, 9, 28].

Design Choices of Affordance-Adaption Module. We start from EVF-SAM without any structural changes and gradually integrate our methods to analyze the effect of each proposed design in affordance-adaption module. The results in Tab 4 reveal that each element consistently delivers

Num.	KLD ↓	SIM ↑	NSS ↑
1	1.408	0.358	1.562
2	1.198	0.503	1.700
3	1.128	0.514	1.761

Table 5. **Ablation results of number of filtration.** Num. indicates the number of times we filter the affordance maps shown in steps 4~6 of Algorithm 1.

γ	KLD ↓	SIM ↑	NSS ↑
0	1.394	0.387	1.693
0.3	1.248	0.455	1.681
0.45	1.128	0.514	1.761
0.6	1.302	0.432	1.628
0.9	1.360	0.410	1.497

Table 6. **Ablation results of γ .** γ indicates the intensity of filtration when we post-process affordance maps produced by LOCATE.

notable improvements. In particular, we notice that adding learnable queries benefits a lot, which is in line with findings in other works [18, 22, 57] that use prompt learning when adapting a foundation model to downstream tasks.

Effect of Post-Processing Program. As we display in the first two columns of Figure 6, the quality of affordance maps directly output by LOCATE is sometimes terrible, which would result in corruption of the model capability supervised on these maps (see Table 6 when $\gamma = 0$). By contrast, after processing with an optimal filtration intensity of $\gamma = 0.45$ and number of 3 (see Table 5), most of the irrelevant areas are eliminated, while areas related to the functional part are preserved (see the second two columns of Figure 6). This optional design choose also leads to a significant performance improvement across all metrics.

5. Conclusion

In this paper, we introduce AffordanceSAM, a new state-of-the-art affordance grounding model. Built upon EVF-SAM with our proposed affordance-adaption module, AffordanceSAM demonstrates superior performance in affordance grounding tasks after a systematically designed coarse-to-fine training. The zero-shot affordance grounding evaluation on internet images further demonstrates the generalization capacity of AffordanceSAM. Despite AffordanceSAM still has its constraints, such as the suboptimal performance in complex scenarios (see Appendix 7), we still believe AffordanceSAM can become the new baseline for subsequent studies and offer timely insights into how to leverage and extend SAM-like foundation models to benefit more relevant vision tasks with limited labeled data resources.

References

- [1] Paola Ardón, Eric Pairet, Ronald PA Petrick, Subramanian Ramamoorthy, and Katrin S Lohan. Learning grasp affordance reasoning through semantic relations. *IEEE Robotics and Automation Letters*, 4(4):4571–4578, 2019. 12
- [2] Paola Ardón, Èric Pairet, Katrin S Lohan, Subramanian Ramamoorthy, and Ronald Petrick. Affordances in robotic tasks—a survey. *arXiv preprint arXiv:2004.07400*, 2020. 12
- [3] Shikhar Bahl, Russell Mendonca, Lili Chen, Unnat Jain, and Deepak Pathak. Affordances from human videos as a versatile representation for robotics. In *Proceedings of the IEEE/CVF Conference on Computer Vision and Pattern Recognition*, pages 13778–13790, 2023. 12
- [4] Jinze Bai, Shuai Bai, Shusheng Yang, Shijie Wang, Sinan Tan, Peng Wang, Junyang Lin, Chang Zhou, and Jingren Zhou. Qwen-vl: A versatile vision-language model for understanding, localization. *Text Reading, and Beyond*, 2, 2023. 8
- [5] Homanga Bharadhwaj, Abhinav Gupta, and Shubham Tulsiani. Visual affordance prediction for guiding robot exploration. In *2023 IEEE International Conference on Robotics and Automation (ICRA)*, pages 3029–3036. IEEE, 2023. 12
- [6] Jessica Borja-Diaz, Oier Mees, Gabriel Kalweit, Lukas Hermann, Joschka Boedecker, and Wolfram Burgard. Affordance learning from play for sample-efficient policy learning. In *2022 International Conference on Robotics and Automation (ICRA)*, pages 6372–6378. IEEE, 2022. 12
- [7] Zoya Bylinskii, Tilke Judd, Aude Oliva, Antonio Torralba, and Frédo Durand. What do different evaluation metrics tell us about saliency models? *IEEE transactions on pattern analysis and machine intelligence*, 41(3):740–757, 2018. 5, 12
- [8] Nicolas Carion, Francisco Massa, Gabriel Synnaeve, Nicolas Usunier, Alexander Kirillov, and Sergey Zagoruyko. End-to-end object detection with transformers. In *European conference on computer vision*, pages 213–229. Springer, 2020. 4
- [9] Zhe Chen, Weiyun Wang, Hao Tian, Shenglong Ye, Zhangwei Gao, Erfei Cui, Wenwen Tong, Kongzhi Hu, Jiapeng Luo, Zheng Ma, et al. How far are we to gpt-4v? closing the gap to commercial multimodal models with open-source suites. *Science China Information Sciences*, 67(12):220101, 2024. 8
- [10] A Conneau. Unsupervised cross-lingual representation learning at scale. *arXiv preprint arXiv:1911.02116*, 2019. 13
- [11] Golnaz Ghiasi, Yin Cui, Aravind Srinivas, Rui Qian, Tsung-Yi Lin, Ekin D. Cubuk, Quoc V. Le, and Barret Zoph. Simple copy-paste is a strong data augmentation method for instance segmentation. In *Proceedings of the IEEE/CVF Conference on Computer Vision and Pattern Recognition*, pages 2918–2928, 2021. 12
- [12] James J Gibson. *The ecological approach to visual perception: classic edition*. Psychology press, 2014. 1, 2
- [13] Andrew Guo, Bowen Wen, Jianhe Yuan, Jonathan Tremblay, Stephen Tyree, Jeffrey Smith, and Stan Birchfield. Handal: A dataset of real-world manipulable object categories with pose annotations, affordances, and reconstructions. In *2023 IEEE/RSJ International Conference on Intelligent Robots and Systems (IROS)*, pages 11428–11435. IEEE, 2023. 4, 12
- [14] Guangxing Han and Ser-Nam Lim. Few-shot object detection with foundation models. In *Proceedings of the IEEE/CVF Conference on Computer Vision and Pattern Recognition*, pages 28608–28618, 2024. 2, 3
- [15] Mohammed Hassanin, Salman Khan, and Murat Tahtali. Visual affordance and function understanding: A survey. *ACM Computing Surveys (CSUR)*, 54(3):1–35, 2021. 1, 2
- [16] Sahar Kazemzadeh, Vicente Ordonez, Mark Matten, and Tamara Berg. Referitgame: Referring to objects in photographs of natural scenes. In *Proceedings of the 2014 conference on empirical methods in natural language processing (EMNLP)*, pages 787–798, 2014. 4
- [17] Lei Ke, Mingqiao Ye, Martin Danelljan, Yu-Wing Tai, Chi-Keung Tang, Fisher Yu, et al. Segment anything in high quality. *Advances in Neural Information Processing Systems*, 36, 2024. 4, 12
- [18] Muhammad Uzair Khattak, Syed Talal Wasim, Muzammal Naseer, Salman Khan, Ming-Hsuan Yang, and Fahad Shahbaz Khan. Self-regulating prompts: Foundational model adaptation without forgetting. In *Proceedings of the IEEE/CVF International Conference on Computer Vision*, pages 15190–15200, 2023. 2, 3, 8
- [19] Diederik P Kingma. Adam: A method for stochastic optimization. *arXiv preprint arXiv:1412.6980*, 2014. 5
- [20] Alexander Kirillov, Eric Mintun, Nikhila Ravi, Hanzi Mao, Chloe Rolland, Laura Gustafson, Tete Xiao, Spencer Whitehead, Alexander C Berg, Wan-Yen Lo, et al. Segment anything. In *Proceedings of the IEEE/CVF International Conference on Computer Vision*, pages 4015–4026, 2023. 2, 3, 5, 12, 13
- [21] Mia Kokic, Johannes A Stork, Joshua A Haustein, and Danica Kragic. Affordance detection for task-specific grasping using deep learning. In *2017 IEEE-RAS 17th International Conference on Humanoid Robotics (Humanoids)*, pages 91–98. IEEE, 2017. 12
- [22] Marc Lafon, Elias Ramzi, Clément Rambour, Nicolas Audibert, and Nicolas Thome. Gallop: Learning global and local prompts for vision-language models. *arXiv preprint arXiv:2407.01400*, 2024. 8
- [23] Xin Lai, Zhuotao Tian, Yukang Chen, Yanwei Li, Yuhui Yuan, Shu Liu, and Jiaya Jia. Lisa: Reasoning segmentation via large language model. In *Proceedings of the IEEE/CVF Conference on Computer Vision and Pattern Recognition*, pages 9579–9589, 2024. 3, 12, 14
- [24] Gen Li, Varun Jampani, Deqing Sun, and Laura Sevilla-Lara. Locate: Localize and transfer object parts for weakly supervised affordance grounding. In *Proceedings of the IEEE/CVF Conference on Computer Vision and Pattern Recognition*, pages 10922–10931, 2023. 1, 3, 5, 14
- [25] Gen Li, Deqing Sun, Laura Sevilla-Lara, and Varun Jampani. One-shot open affordance learning with foundation models. In *Proceedings of the IEEE/CVF Conference on Computer*

- Vision and Pattern Recognition*, pages 3086–3096, 2024. 1, 2, 3, 5, 6, 14
- [26] Junnan Li, Dongxu Li, Silvio Savarese, and Steven Hoi. Blip-2: Bootstrapping language-image pre-training with frozen image encoders and large language models. In *International conference on machine learning*, pages 19730–19742. PMLR, 2023. 4
- [27] T Lin. Focal loss for dense object detection. *arXiv preprint arXiv:1708.02002*, 2017. 5
- [28] Haotian Liu, Chunyuan Li, Qingyang Wu, and Yong Jae Lee. Visual instruction tuning. *Advances in neural information processing systems*, 36:34892–34916, 2023. 8, 12, 14
- [29] Hongchen Luo, Wei Zhai, Jing Zhang, Yang Cao, and Dacheng Tao. Learning affordance grounding from exocentric images. In *Proceedings of the IEEE/CVF conference on computer vision and pattern recognition*, pages 2252–2261, 2022. 1, 3, 5, 12, 14
- [30] Teli Ma, Zifan Wang, Jiaming Zhou, Mengmeng Wang, and Junwei Liang. Glover: Generalizable open-vocabulary affordance reasoning for task-oriented grasping. *arXiv preprint arXiv:2411.12286*, 2024. 12
- [31] Jinjie Mai, Meng Yang, and Wenfeng Luo. Erasing integrated learning: A simple yet effective approach for weakly supervised object localization. In *Proceedings of the IEEE/CVF conference on computer vision and pattern recognition*, pages 8766–8775, 2020. 2
- [32] Shervin Minaee, Yuri Boykov, Fatih Porikli, Antonio Plaza, Nasser Kehtarnavaz, and Demetri Terzopoulos. Image segmentation using deep learning: A survey. *IEEE transactions on pattern analysis and machine intelligence*, 44(7):3523–3542, 2021. 2
- [33] Austin Myers, Ching L Teo, Cornelia Fermüller, and Yiannis Aloimonos. Affordance detection of tool parts from geometric features. In *2015 IEEE International Conference on Robotics and Automation (ICRA)*, pages 1374–1381. IEEE, 2015. 4, 12
- [34] Tushar Nagarajan, Christoph Feichtenhofer, and Kristen Grauman. Grounded human-object interaction hotspots from video. In *Proceedings of the IEEE/CVF International Conference on Computer Vision*, pages 8688–8697, 2019. 1, 2
- [35] Maxime Oquab, Timothée Darcet, Théo Moutakanni, Huy Vo, Marc Szafraniec, Vasil Khalidov, Pierre Fernandez, Daniel Haziza, Francisco Massa, Alaaeldin El-Nouby, et al. Dinov2: Learning robust visual features without supervision. *arXiv preprint arXiv:2304.07193*, 2023. 3, 14
- [36] Kingjia Pan, Yingguo Gao, Zhiwen Lin, Fan Tang, Weiming Dong, Haolei Yuan, Feiyue Huang, and Changsheng Xu. Unveiling the potential of structure preserving for weakly supervised object localization. In *Proceedings of the IEEE/CVF conference on computer vision and pattern recognition*, pages 11642–11651, 2021. 2
- [37] Robert J Peters, Asha Iyer, Laurent Itti, and Christof Koch. Components of bottom-up gaze allocation in natural images. *Vision research*, 45(18):2397–2416, 2005. 5, 12
- [38] Shengyi Qian and David F Fouhey. Understanding 3d object interaction from a single image. In *Proceedings of the IEEE/CVF International Conference on Computer Vision*, pages 21753–21763, 2023. 1, 2
- [39] Shengyi Qian, Weifeng Chen, Min Bai, Xiong Zhou, Zhuowen Tu, and Li Erran Li. Affordancellm: Grounding affordance from vision language models. In *Proceedings of the IEEE/CVF Conference on Computer Vision and Pattern Recognition*, pages 7587–7597, 2024. 1, 2, 3, 5, 12, 14
- [40] Alec Radford, Jong Wook Kim, Chris Hallacy, Aditya Ramesh, Gabriel Goh, Sandhini Agarwal, Girish Sastry, Amanda Askell, Pamela Mishkin, Jack Clark, et al. Learning transferable visual models from natural language supervision. In *International conference on machine learning*, pages 8748–8763. PMLR, 2021. 3, 14
- [41] Nikhila Ravi, Valentin Gabeur, Yuan-Ting Hu, Ronghang Hu, Chaitanya Ryali, Tengyu Ma, Haitham Khedr, Roman Rädle, Chloe Rolland, Laura Gustafson, et al. Sam 2: Segment anything in images and videos. *arXiv preprint arXiv:2408.00714*, 2024. 2, 5, 12, 13
- [42] Tianhe Ren, Shilong Liu, Ailing Zeng, Jing Lin, Kunchang Li, He Cao, Jiayu Chen, Xinyu Huang, Yukang Chen, Feng Yan, et al. Grounded sam: Assembling open-world models for diverse visual tasks. *arXiv preprint arXiv:2401.14159*, 2024. 3
- [43] Usha Ruby and Vamsidhar Yendapalli. Binary cross entropy with deep learning technique for image classification. *Int. J. Adv. Trends Comput. Sci. Eng*, 9(10), 2020. 4
- [44] Christoph Schuhmann, Richard Vencu, Romain Beaumont, Robert Kaczmarczyk, Clayton Mullis, Aarush Katta, Theo Coombes, Jenia Jitsev, and Aran Komatsuzaki. Laion-400m: Open dataset of clip-filtered 400 million image-text pairs. *arXiv preprint arXiv:2111.02114*, 2021. 4
- [45] Carole H Sudre, Wenqi Li, Tom Vercauteren, Sebastien Ourselin, and M Jorge Cardoso. Generalised dice overlap as a deep learning loss function for highly unbalanced segmentations. In *Deep Learning in Medical Image Analysis and Multimodal Learning for Clinical Decision Support: Third International Workshop, DLMIA 2017, and 7th International Workshop, ML-CDS 2017, Held in Conjunction with MICCAI 2017, Québec City, QC, Canada, September 14, Proceedings 3*, pages 240–248. Springer, 2017. 4
- [46] Michael J Swain and Dana H Ballard. Color indexing. *International journal of computer vision*, 7(1):11–32, 1991. 5, 12
- [47] Mengmeng Wang, Jiazheng Xing, Jianbiao Mei, Yong Liu, and Yunliang Jiang. Actionclip: Adapting language-image pretrained models for video action recognition. *IEEE Transactions on Neural Networks and Learning Systems*, 2023. 2, 3
- [48] Wenhui Wang, Hangbo Bao, Li Dong, Johan Bjorck, Zhiliang Peng, Qiang Liu, Kriti Aggarwal, Owais Khan Mohammed, Saksham Singhal, Subhojit Som, et al. Image as a foreign language: Beit pretraining for vision and vision-language tasks. In *Proceedings of the IEEE/CVF Conference on Computer Vision and Pattern Recognition*, pages 19175–19186, 2023. 3, 13
- [49] Xintong Yang, Ze Ji, Jing Wu, and Yu-Kun Lai. Recent advances of deep robotic affordance learning: a reinforcement learning perspective. *IEEE Transactions on Cognitive and Developmental Systems*, 15(3):1139–1149, 2023. 12

- [50] Licheng Yu, Patrick Poirson, Shan Yang, Alexander C Berg, and Tamara L Berg. Modeling context in referring expressions. In *Computer Vision—ECCV 2016: 14th European Conference, Amsterdam, The Netherlands, October 11–14, 2016, Proceedings, Part II 14*, pages 69–85. Springer, 2016. [4](#)
- [51] Wei Zhai, Hongchen Luo, Jing Zhang, Yang Cao, and Dacheng Tao. One-shot object affordance detection in the wild. *International Journal of Computer Vision*, 130(10): 2472–2500, 2022. [4](#), [12](#)
- [52] Yuxuan Zhang, Tianheng Cheng, Rui Hu, Heng Liu, Longjin Ran, Xiaoxin Chen, Wenyu Liu, Xinggang Wang, et al. Evfsam: Early vision-language fusion for text-prompted segment anything model. *arXiv preprint arXiv:2406.20076*, 2024. [3](#), [5](#)
- [53] Rui Zhao, Yuchao Gu, Jay Zhangjie Wu, David Junhao Zhang, Jiawei Liu, Weijia Wu, Jussi Keppo, and Mike Zheng Shou. Motiondirector: Motion customization of text-to-video diffusion models. *arXiv preprint arXiv:2310.08465*, 2023. [2](#), [3](#)
- [54] Xu Zhao, Wenchao Ding, Yongqi An, Yinglong Du, Tao Yu, Min Li, Ming Tang, and Jinqiao Wang. Fast segment anything. *arXiv preprint arXiv:2306.12156*, 2023. [3](#)
- [55] Zhong-Qiu Zhao, Peng Zheng, Shou-tao Xu, and Xindong Wu. Object detection with deep learning: A review. *IEEE transactions on neural networks and learning systems*, 30(11):3212–3232, 2019. [2](#)
- [56] Bolei Zhou, Aditya Khosla, Agata Lapedriza, Aude Oliva, and Antonio Torralba. Learning deep features for discriminative localization. In *Proceedings of the IEEE conference on computer vision and pattern recognition*, pages 2921–2929, 2016. [2](#)
- [57] Kaiyang Zhou, Jingkang Yang, Chen Change Loy, and Ziwei Liu. Learning to prompt for vision-language models. *International Journal of Computer Vision*, 130(9):2337–2348, 2022. [2](#), [8](#)

Appendix of AffordanceSAM

Table 8. Statistics of datasets we used in each stage. Part: part-level annotation. Obj.: number of object classes. Aff: number of affordance function classes. Img.: number of images.

Dataset	Year	Part	Obj.	Aff.	Img.
<i>Stage1</i>					
PADv2 [51]	2021	×	103	39	30,000
RGB-D Part Affordance [33]	2022	✓	37	15	47,210
Handal [13]	2023	✓	212	17	30,800
<i>Stage2 and Stage3</i>					
AGD20k [29]	2021	✓	50	36	23,816

1. More Discussion on Related Work

Affordance learning for robotics. Recently, Numerous methodologies have been developed by researchers to extract and interpret affordance information to enable the robots to grasp in a complex, dynamic environments [2, 49]. Specifically, several studies [1, 21, 30] leverage affordance to establish correlations between objects, tasks, and manipulation strategies for robotic grasping. Other studies [3, 5, 6] focus on deriving affordance knowledge from resources that can be deployed on real robotic systems. In this study, we only focus on the visual affordance grounding task, and our main insight is taking advantage of SAM’s generalization ability to compensate for the deficiencies of the previous methods. But we also believe our propose AffordanceSAM can greatly improve the robot’s ability to recognize and grasp objects and becomes a default option for robot deployment by other researchers.

Segment anything model and its extension. The Segment Anything Model (SAM) [20, 41] is an interactive segmentation framework that produces binary masks in response to various prompt types (points, boxes, and coarse masks). Trained on a comprehensive dataset, SAM exhibits robust generalization capacity for segmenting diverse objects. Building upon SAM, SAM-HQ [17] addresses the segmentation quality of SAM by introducing a set of hq-tokens; LISA [23] combines SAM with LLaVA [28] to enable segmentation model with reasoning ability. Our work also start from SAM, but we focus on converting SAM to be a generalized affordance grounding model with our proposed affordance-adaption module and coarse-to-fine training recipe.

2. More Details about Our Datasets

Here we provide the detailed dataset setup for training and testing AffordanceSAM. The statistics of each dataset is provided in Table 8.

Stage1. In this stage, we use PADv2 [51], Handal [13], and RGB-D Part Affordance [33]. All three datasets are com-

posed of different object and affordance categories, and images of the same affordance and category are treated as one class. The ground-truth of three datasets is binary mask, but a slight different is that Handal and RGB-D Part Affordance label the part of the object according to the affordance action, and PADv2 only gives the mask of the whole object. Moreover, as Handal and RGB-D Part Affordance are obtained from continuous frames of videos, which means many of the images of same object category are very similar. We randomly sampled 5 images for those belong to a video clip to avoid potential over-fitting problem. And for PADv2, we filter duplicate images and add remaining images in our training data. Noticing that we do not split any object in this stage like in stage2 and stage3, because the output form of this stage is completely different from the output used in the final evaluation.

Stage2 and stage3. In these two stages, we strictly follow AffordanceLLM [39] to split AGD20K [29] for training and testing our model. The easy split is the original unseen split of AGD20K, which has a lot of similarities between the objects in the train and test sets. The hard split ensures that there is no overlap between the object categories in the train and test set. This setting can help to reflect the model generalization ability when the similarity between the training data and the test data changes. More details can be found in AffordanceLLM’s paper and project².

3. More Details about Implementation

In this section, we provide specific training hyperparameters in each stage and model configuration of different version of AffordanceSAM in Table 9 and Table 10, respectively.

What’s more, we use different data augmentation when training AffordanceSAM_{SAM1} (large-scale jitter [11] with a scale range of [0.1, 2.0], rand-hflip with a ratio of 0.5) and AffordanceSAM_{SAM2} (only rand-hflip with a ratio of 0.5), because we find that using the data augmentation in accordance with that used in the backbone’s pre-training [20, 41] can lead to better results. We use the checkpoint after the whole training in first two stages as the initialization of the next stage.

4. Details of Each Metrics for Evaluation

In this section, we explain the metrics (KLD [7], SIM [46], and NSS [37]) to evaluate models.

- **Kullback-Leibler Divergence (KLD)** measures distribution difference between the predicted affordance map (M)

²<https://jasonqsy.github.io/AffordanceLLM/>

Table 9. Training hyperparameters of AffordanceSAM in each stage.

Name	Stage1	Stage2	Stage3
Learning rate	2e-5	2e-5	4e-5
Learning rate scheduler	Cosine decay	Cosine decay	Cosine decay
Epochs	13	13	26
LR warmup epochs	1	2	0
Total batch size	32	32	32
Optimizer	AdamW	AdamW	AdamW
AdamW - β_1	0.9	0.9	0.9
AdamW - β_2	0.999	0.999	0.999
Drop path	0.1	0.1	0.1
Gradient clip	3	3	3
λ_{dice}	0.5	–	–
λ_{bce}	1	–	–
Seed	42	42	42

Name	AffordanceSAM _{SAM1}	AffordanceSAM _{SAM2}
<i>Segmentation Model</i>		
Encoder&Decoder	SAM-ViT-H [20]	SAM2-hiera-L [41]
Image input size	1024×1024	1024×1024
Patch size	16	16
Encoder hidden dimension	1280	576
Global attention blocks	[7, 15, 23, 31]	[23, 33, 43]
<i>Multimodal Model</i>		
Encoder	BEIT-3-L [48]	BEIT-3-L [48]
Text tokenizer	XLM-Roberta [10]	XLM-Roberta [10]
Image input size	224×224	224×224
Patch size	16	16
Encoder hidden dimension	1024	1024

Table 10. Model configuration of AffordanceSAM.

and the ground truth (M'), which is

$$\text{KLD}(M, M') = \sum_i M'_i \log \left(\epsilon + \frac{M'_i}{\epsilon + M_i} \right), \quad (6)$$

• **Similiary (SIM)** is also called histogram intersection, which measures the intersection between the predicted affordance map (M) and the ground truth (M'). The final range is from 0 to 1. It is given by

$$\text{SIM}(M, M') = \sum_i \min(M_i, M'_i), \quad (7)$$

where $\sum_i M_i = \sum_i M'_i = 1$.

• **Normalized Scanpath Saliency (NSS)** measures the correspondence between the prediction map (M) and the ground truth (M'). It is given by

$$\text{NSS}(M, M') = \frac{1}{N} \sum_i \hat{M} \times M'_i, \quad (8)$$

where $N = \sum_i M'_i$, $\hat{M} = \frac{M - \mu(M)}{\sigma(M)}$. $\mu(M)$ and $\sigma(M)$ are the mean and standard deviation, respectively.

5. Methods for Comparison

Affordance grounding methods can be mainly summarized into two main categories: weakly supervised and fully supervised methods. For weakly supervised models, they do not train on explicit labels of the affordance map. Instead, they are trained on two views (egocentric and exocentric) of the same object. As for fully supervised models, they are supervised under dense labels. In what follows, we explain the main idea of baseline methods that we used for the evaluation and comparison.

Cross-View-AG [29] proposes a novel framework to extract invariant affordance from exocentric interactions and transfer it to egocentric views. This includes an Affordance Invariance Mining module to minimize intra-class differences in exocentric images and an Affordance Co-relation Preserving strategy to align co-relation matrices between views for affordance perception and localization.

LOCATE [24] first localizes where the interaction happens and identifies interaction regions in exocentric views, then uses a PartSelect module to extract affordance-specific information, and transfers this knowledge to egocentric views for affordance grounding using only image-level labels.

AffordanceLLM [39] leverages LLaVA [28] with a new mask token similar to LISA [23] and introduce depth maps as 3D information to build the main pipeline. A light-weight mask decoder trained from scratch is also introduced to produce affordance map.

OOAL [25] proposes a vision-language framework that includes CLIP [40] and DINOv2 [35]. To boost the alignment between visual features of DINOv2 and affordance text embeddings extracted by CLIP, several light-weight modules like learnable text prompt tokens and a CLS-guided transformer decoder are introduced.

6. More Details about Ablation Setup

In this section, we have a detailed illustration of the evaluation setup of each table in our ablation study. The table index here refers to the index in the main paper.

Table 3. This table presents the effect of our proposed coarse-to-fine training recipe. The first line of results is obtained by directly using EVF-SAM’s checkpoint³ to evaluate. Then we gradually add the training data divided by stage and use the last checkpoint to evaluate. When combining all the data, we add affordance-adaption module at the beginning of the training, which is a slightly different from our default setting.

Table 4. This table presents the effect of each component in our proposed affordance-adaption module. The learnable queries in the second row do not conduct any cross-attention with mentioned features but conduct self-attention twice as we mentioned in Section 3.2 in the main paper.

³<https://github.com/hustvl/EVF-SAM>

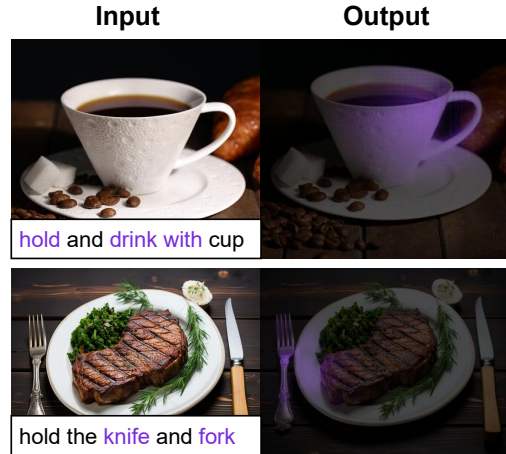


Figure 7. Failure cases when facing multiple objects or multiple affordance functions.

Table 5 and Table 6. These two tables present the effect of design choice of our proposed post-processing program. In first row of Table 5, we do not use the 5~6 steps in Algorithm 1. And so on for the second and third rows. Noticing that we only vary five values of γ results in Table 6, we believe more optional value of γ can be further searched; however, given the constraints of time and computational resources, as well as the diminishing returns on additional searches, we have decided not to pursue further searches. This decision does not affect the significance of our contribution.

7. Failure Cases and Feature Work

Although our AffordanceSAM achieves state-of-the-art (SOTA) performance under the AGD20K benchmark, and generalized well beyond the training data, when faced with more complex scenarios (e.g. multi-objects affordance), it sometimes cannot get accurate results. As shown in Figure 7, first, we find AffordanceSAM fails on completely separating two different functional regions of an object when prompted with multi-actions (see the first row of Figure 7). Next, we find that AffordanceSAM can not get an accurate affordance map when two different objects in a picture but prompted with the same affordance action (see the second row of Figure 7). These limitations may be caused by the fact that every image we use to train AffordanceSAM is single object format with single affordance region involved.

Thus, endowing AffordanceSAM with the capability to deal with more complex scenarios like multiple objects or multiple affordance functions within a single image might be an exciting avenue for future research and development.